EMT Program is Dispensable for Metastasis but Induces Chemoresistance in Pancreatic Cancer

Xiaofeng Zheng[#1], **Julienne L. Carstens**[#1], **Jiha Kim**[1], **Matthew Scheible**[1], **Judith Kaye**[1], **Hikaru Sugimoto**[1], **Chia-Chin Wu**[2], **Valerie S. LeBleu**[1], and **Raghu Kalluri**[1,3,4]

[1]Department of Cancer Biology, Metastasis Research Center, University of Texas MD Anderson Cancer Center, Houston, Texas

[2]Department of Genomic Medicine, University of Texas MD Anderson Cancer Center, Houston, Texas

[3]Department of Molecular and Cellular Biology, Baylor College of Medicine, Houston, Texas

[4]Department of Bioengineering, Rice University, Houston, Texas.

[#] These authors contributed equally to this work.

Diagnosis of pancreatic ductal adenocarcinoma (PDAC) is associated with dismal prognosis despite current therapies; therefore new treatment strategies are urgently required. Numerous studies have suggested that epithelial to mesenchymal transition (EMT) contributes to early-stage dissemination of cancer cells and is pivotal for invasion and metastasis of PDAC[1-4]. EMT program is associated with phenotypic conversion of epithelial cells into mesenchymal-like cells in cell culture conditions, albeit such defined mesenchymal conversion (with spindle shaped morphology) of epithelial cells is rare with quasi-mesenchymal phenotypes occasionally observed in the tumor (partial EMT)[5,6]. Most studies exploring the functional role of EMT in tumors have depended on cell culture induced loss-of-function and gain-of-function experiments involving EMT inducing transcription factors such as Twist, Snail and Zeb1[2,3,7-10]. Therefore, the functional contribution of EMT program for invasion and metastasis remains unclear[4,6] and genetically engineered mouse models (GEMMs) to specifically address a causal connection are lacking. Here we functionally probed the role of EMT program in PDAC by generating PDAC GEMMs with deletion of Snail or Twist, two key transcription factors responsible for EMT. EMT suppression in the primary tumor did not alter the emergence of invasive PDAC, systemic

dissemination and metastasis. Suppression of EMT led to an increase in cancer cell proliferation with enhanced expression of nucleoside transporters in tumors, contributing to enhanced sensitivity to gemcitabine treatment and increased overall survival of mice. Collectively, our study suggests that Snail or Twist induced EMT program is not rate-limiting for invasion and metastasis but highlights the importance of combining EMT inhibition with chemotherapy for the treatment of pancreatic cancer.

We crossed *Twist1*$^{L/L}$ or *Snai1*$^{L/L}$ mice with *Pdx1-Cre; LSL-Kras*^{G12D}; *P53*$^{R172H/+}$ (KPC) to generate the *Pdx1-Cre; LSL-Kras*^{G12D}; *P53*$^{R172H/+}$; *Twist1*$^{L/L}$ (KPC; Twist^{cKO}) and the *Pdx1-Cre; LSL-Kras*^{G12D}; *P53*$^{R172H/+}$; *Snai1*$^{L/L}$ (KPC; Snail^{cKO}) mice, respectively. The resultant progeny were born in an expected Mendelian ratio, without overt phenotypic findings other than the anticipated emergence of spontaneous pancreatic cancer (**Extended Figure 1A**). Genetic deletion of *Snai1* or *Twist1* did not significantly delay pancreatic tumorigenesis, alter tumor histopathology features or local invasion (**Figure 1A-C** and **Extended Table 1**). KPC; Twist^{cKO} and KPC; Snail^{cKO} mice displayed similar tumor burden compared to KPC control mice (**Extended Figure 1B**), and insignificant difference in overall survival (**Figure 1D**). Loss of *Twist1* or *Snai1* expression in the pancreas epithelium was confirmed by *in situ* hybridization coupled with CK8 epithelial immunolabeling (**Figure 1E** and **Extended Figure 1C**) as well as immunolabeling for Twist and Snail (**Extended Figure 1D**). Suppression of EMT program was significantly noted (**Figure 1F-G, Extended Figure 1E**). Lineage tracing (**Figure 1F**) and immunolabeling of the primary tumor (**Figure 1G**) showed a significant decrease in the frequency of epithelial cells with expression of the mesenchymal marker αSMA (EMT$^+$ cells) and a decrease in expression of EMT inducing transcription factor, Zeb1 (**Figure 1H**). Global gene expression profiling of tumors revealed a decrease in expression of EMT associated genes (including *Snai1* and *Twist1*) in KPC; Snail^{cKO} and KPC; Twist^{cKO} mice compared to KPC control (**Extended Figure 1F**). Loss of Snail and Twist enhanced E-cadherin expression and suppressed Zeb2 and Sox4 expression in cancer cells (**Extended Figure 2A-C**). Snai2 (Slug) expression was restricted to early PanIN lesion in all the experimental groups with no observed expression in advanced tumors and was significantly reduced in KPC; Snail^{cKO} and KPC;Twist^{cKO} mice compared to KPC control mice (**Extended Figure 2D**).

While desmoplasia, including extracellular matrix (ECM) and myofibroblasts content (**Figure 1I** and **Extended Figure 2E-F**), tumor vessel density (**Extended Figure 2G**), intratumoral hypoxia (**Extended Figure 2H**), CD3$^+$ T-cell infiltration (**Extended Figure 2I**), and cancer cell apoptosis was unaffected with Twist/Snail deletion in KPC tumors (**Figure 2A**), the proliferation of cancer cells in mice with suppressed EMT program was significantly increased (**Figure 2B**), as shown previously in mouse models of breast cancers[11-13]. Immunostaining experiments further revealed that EMT$^+$ cancer cells are largely Ki67$^-$ (**Extended Figure 3A**). Altogether, the data suggests that EMT program driven by Twist/Snail transcription factors is dispensable for initiation and progression of primary pancreatic cancer.

Next, we investigated whether suppression of EMT program impacts invasion and metastasis. The number of YFP$^+$ CTCs from lineage traced KPC and KPC; Twist^{cKO} was found unchanged (**Figure 2C** and **Extended Figure 3B**), and expression of cancer cell

specific Kras[G12D] mRNA in the blood from KPC, KPC; Twist[cKO] and KPC; Snail[cKO] was unaffected (**Figure 2D**), suggesting that suppression of EMT program in pancreatic tumors does not impact the rate of systemic dissemination of cancer cells. Extensive histopathological analyses, coupled with CK19 or YFP immunostaining of distant metastatic target organs, namely the liver, lung and spleen, indicated a similar frequency of metastasis in EMT suppressed tumors when compared to control tumors (**Figure 2E, Extended Figure 3C, Extended Table 1**, and **Extended Table 2**). The metastases were negative for Twist and Snail, and only a few KPC metastatic cells expressed αSMA or Zeb1 (**Extended Figure 3D-F**), while being positive for E-cadherin and Ki-67 (**Extended Figure 3G-H**). The proliferation rate of cancer cells in the metastases was similar in KPC, KPC; Snail[cKO] and KPC; Twist[cKO] mice (**Extended Figure 3H**). Collectively, the results indicated that the genetic deletion of *Twist1* or *Snail1* in PDAC GEMMs did not reduce metastatic disease.

To evaluate whether cancer cells from the pancreas with and without EMT program differentially benefited from impaired proliferation to form secondary tumors, we isolated cancer cells from KPC, KPC; Twist[cKO] and KPC; Snail[cKO] mice to assay their organ colonization potential. *Twist1* was significantly reduced and *Snail1* expression was undetectable in cancer cells isolated from Twist and Snail deleted tumors, respectively (**Figure 2F**). Short-term potential to form tumor spheres (associated with putative cancer stem phenotype) appeared similar in Twist[cKO] and Snail[cKO] KPC cells when compared to control KPC cells (**Figure 2G**)[3,8,14-16]. Lung colonization frequency following the i.v. injection of KPC cancer cells (Twist or Snail deleted) were similar to the control KPC cancer cells (**Figure 2H**). These results suggest that a favored epithelial phenotype of cancer cells (via suppression of EMT program) did not impact the capacity to form tumor spheres or their ability for organ colonization[17].

Cancer cell EMT program is associated with gemcitabine drug resistance in PDAC patients and in the orthotopic mouse models of PDAC[1,2,8,9,18-23]. Moreover, enhanced frequency of EMT^{+} cancer cells in pancreatic tumors is associated with poor survival[24,25]. To determine whether EMT program suppression enhances PDAC sensitivity to gemcitabine chemotherapy, we tested the gemcitabine sensitivity of cancer cells with suppressed EMT program in KPC mice. Equilibrative nucleoside transporter ENT1 and concentrating nucleoside transporter CNT3 were significantly upregulated in cancer cells lacking Snail and Twist, while ENT2 expression was unchanged (**Figure 3A-C**). KPC, KPC; Snail[cKO] and KPC; Twist[cKO] mice were treated with gemcitabine and tumor burden was monitored by MRI (**Extended Table 3**). Tumor progression was suppressed in KPC; Snail[cKO] and KPC; Twist[cKO] mice when compared to treated KPC control mice (**Figure 3D**). KPC; Snail[cKO] and KPC; Twist[cKO] mice treated with gemcitabine showed improved histopathology and increased survival (**Figure 3E-G**).

Cancer cells isolated from the tumors of KPC; Snail[cKO] and KPC; Twist[cKO] mice showed epithelial morphology (**Extended Figure 4A**) and reduced expression of mesenchymal genes compared to KPC cancer cell lines (**Extended Figure 4B**), however, in tissue culture conditions (2D culture on plastic), equilibrative nucleoside transporters (ENT1/ENT2/ENT3) showed similar expression pattern and expression of concentrating nucleoside transporters (CNT1/CNT3) was not detected (**Extended Figure 4B**). Increased proliferation

of KPC; Snail[cKO] and KPC; Twist[cKO] cancer cells compared to KPC control cells (**Extended Figure 4C**) likely accounted for the increased sensitivity to gemcitabine and erlotinib in this setting (**Extended Figure 4D**).

Next, we crossed the *Snai1[L/L]* to the PDAC GEMM, *Ptf1a (P48)-Cre; LSL-Kras[G12D]; Tgfbr2[L/L]* (KTC) to generate *Ptf1a (P48)-Cre; LSL-Kras[G12D]; Tgfbr2[L/L]; Snai1[L/L]* (KTC; Snail[cKO]). The KTC model offers a reliable and penetrant disease progression rate with a consistent timeline of death due to PDAC. Similar to the KPC; Snail[cKO] mice, KTC; Snail[cKO] deletion exhibited suppression of EMT program but did not impact primary tumor histopathology, lifespan, local invasion, desmoplasia and frequency of apoptosis (**Figure 4F, Extended Figure 5A-E**, and **Extended Figure 6A**). KTC; Snail[cKO] mice presented with significantly reduced Zeb1 expression in cancer cells but enhanced proliferation and concentrating nucleoside transporter 3 (CNT3) expression (**Extended Figure 5E**). ENT2 and ENT1 expression were unchanged in KTC; Snail[cKO] mice compared to KTC mice (**Extended Figure 5E** and **Extended Figure 6A**). KTC; Snail[cKO] mice demonstrated enhanced response to gemcitabine therapy, with significant normal parenchymal area and reduced tumor tissue (**Figure 4A-C**). Gemcitabine therapy in KTC; Snail[cKO] reduced tumor burden (**Figure 4D**) and significantly improved overall survival (**Figure 4E**) of mice when compared to gemcitabine treated control KTC mice. Gemcitabine therapy specifically increased cancer cell apoptosis and removed enhanced proliferation observed in EMT program suppressed tumors (**Figure 4G** and **Extended Figure 5E**), without impacting the desmoplastic reaction (**Extended Figure 6B**). Overall, these results suggested an enhanced sensitivity of EMT^{−} cancer cells to gemcitabine. Both the equilibrative nucleoside transporter 2 (ENT2) and the concentrating nucleoside transporter 3 (CNT3) were upregulated in EMT suppressed tumors (**Figure 4G**). These data support a possible mechanistic connection between EMT program and resistance to chemotherapy in PDAC.

Collectively, our studies provide a comprehensive functional analysis of EMT program in PDAC progression and metastasis. Absence of either *Twist1* or *Snai1* did not alter cancer progression or the capacity for local invasion or metastasis to lung and liver in PDAC GEMMs. Metastasis occurs despite a significant loss of EMT program with either the deletion of Snail or Twist, and in both settings, Zeb1, Sox4, Slug and Zeb2 are also significantly suppressed. Nevertheless, it is likely that other EMT inducing factors may compensate for the loss of Snail or Twist to induce invasion and metastasis. While PDX-1 is expressed during the development of the pancreas (in early pancreatic buds: all three major lineages of the pancreas-ductal, acinar and beta-islets), its expression is largely repressed in the adult exocrine pancreas[26,27]. Therefore, deletion of Snail or Twist occurs at the embryonic stage and mice are born normal and exhibit normal pancreas histology prior to the onset of cancer. The GEMMs with Snail or Twist deletion develop PanIN lesions at the same frequency as the control mice. One could argue that suppression of EMT program starting from the inception of cancer could have launched compensatory mechanisms to overcome EMT program-dependent invasion and metastasis. However, such compensation is not observed with respect to chemo-resistance and previous studies have demonstrated that EMT program and cancer cell dissemination are observed even before PDAC lesions are detected in KPC mice[4].

Our study demonstrates that EMT program results in suppression of cancer cell proliferation, and suppression of drug transporter and concentrating proteins, therefore, inadvertently protecting EMT^{+} cells from anti-proliferative drugs such as gemcitabine. The correlation of decreased survival of pancreatic cancer patients with an increased EMT program is likely due to their impaired capacity to respond to gemcitabine, which is a standard of care for most patients[28,29]. Such diminished response to Gemcitabine will likely reflect on such patients also exhibiting higher metastatic disease. Collectively, our study offers the opportunity to evaluate the potential of targeting EMT program to enhance efficacy of Gemcitabine and targeted therapies[30].

Methods

Mice

Characterization of disease progression and genotyping for the *Pdx1-Cre; LSL-Kras^{G12D}; P53$^{R172H/+}$* (herein referred to as KPC) and *Ptf1a (P48)-Cre; LSL-Kras^{G12D}; Tgfbr2$^{L/L}$* (herein referred to as KTC) mice were previously described[31-33]. These mice were bred to *Snai1$^{L/L}$* (herein referred to as Snail^{cKO}), *Twist1$^{L/L}$* (herein referred to as Twist^{cKO}), and *R26-LSL-EYFP*[33]. Snail^{cKO} mice were kindly provided by S.J. Weiss, University of Michigan, Ann Arbor. Twist^{cKO} mice were kindly provided by R. R. Behringer (UT MDACC, Houston, TX) via the Mutant Mouse Regional Resource Center (MMRRC) repository. The resulting progeny were referred to as KPC, KPC; Snail^{cKO}, KPC; Twist^{cKO}, KTC, and KTC; Snail^{cKO} mice and were maintained on a mixed genetic background. Both males and females were used indiscriminately. Mice were given Gemcitabine (G-4177, LC Laboratories) via intraperitoneal injection (i.p.) every other day at 50 mg/kg of body weight. Hypoxyprobe was injected in a subset of mice i.p. at 60 mg/kg of body weight 30 minutes prior to euthanasia. For *in vivo* colonization assay, one million KPC, KPC; Twist^{cKO} and KPC; Snail^{cKO} tumor cells in 100 μL of PBS were injected intravenously via the retro-orbital venous sinus. Four to eleven mice were injected per cell line. All mice were euthanized at 15 days post-injection. All mice were housed under standard housing conditions at MD Anderson Cancer Center (MDACC) animal facilities, and all animal procedures were reviewed and approved by the MDACC Institutional Animal Care and Use Committee. Tumor growth met the standard of a diameter less than or equal to 1.5 cm. Investigators were not blinded for group allocation but were blinded for the assessment of the phenotypic outcome assessed by histological analyses. No randomization method or statistical sample size estimation was used.

Histology and histopathology

Histology, histopathological scoring, Masson's Trichrome staining (MTS), and Picrosirius Red were previously described[19,33]. Formalin-fixed tissues were embedded in paraffin and sectioned at 5 μm thickness. MTS was performed using Gomori's Trichome Stain Kit (38016SS2, Leica Biosystems). Picrosirius red staining for collagen was performed using 0.1% picrosirius red (Direct Red80; Sigma) and counterstained with Weigert's hematoxylin. Sections were also stained with hematoxylin and eosin (H&E). Histopathological measurements were assessed by scoring H&E stained tumors for relative percentages of each histopathological phenotype: normal (non-neoplastic), PanIN, well-differentiated

PDAC, moderately-differentiated PDAC, poorly-differentiated PDAC, sarcomatoid carcinoma, or necrosis. When tumor histology was missing or of poor quality, the mice were excluded from all analyses and this was determined blinded from genotype information. A histological invasion score of the tumor cells into the surrounding stroma was scored on a scale of 0 to 2, with 0 indicating no invasion and 2 indicating high invasion, where invasion is defined as tumor cell dissemination throughout the stroma away from clearly defined epithelial "nests". Microscopic metastases were observed in H&E stained tissue sections of the liver, lung and spleen. Positivity (one or more lesions in a tissue) was confirmed using CK19 and YFP immunohistochemistry. This data has been presented as a contingency table (**Figure 2E**) and represented as the number of positive tissues out of the number of tissues scored. The "Any" metastasis score is the number of mice positive for a secondary lesion found anywhere throughout the body out of the total number of mice scored.

Immunohistochemistry and Immunofluorescence

Tissues were fixed in 10% formalin overnight, dehydrated, and embedded in paraffin and 5 μm thick sections were then processed for analyses. Immunohistochemical analysis was performed as described[33]. Heat mediated antigen retrieval in 1 mM EDTA + 0.05% Tween20 (pH 8.0) for one hour (pressure cooker) was performed for Snail and Twist, 10 mM citrate buffer, pH 6.0 was performed for one hour (microwave) for Ki67 or 10 minutes for all other antibodies. Primary antibodies are as follows: αSMA (M0851, DAKO, 1:400 or ab5694, Abcam, 1:400), cleaved caspase-3 (9661, Cell Signaling, 1:200), CD3 (A0452, DAKO, 1:200), CD31 (Dia310M, DiaNova, 1:10), CK8 (TROMA-1, Developmental Studies Hybridoma Bank, 1:50), CK19 (ab52625, Abcam, 1:100), CNT3 (HPA023311, Sigma-Aldrich, 1:400), ENT1 (LS-B3385, LifeSpan Bio., 1:100), E-cadherin (3195S, Cell Signaling, 1:400), ENT2 (ab48595, Abcam, 1:200), Ki67 (RM-9106, Thermo Scientific, 1:400), SLUG (9585, Cell Signaling, 1:200), SNAIL (ab180714, Abcam, 1:100), SOX4 (ab86809, Abcam, 1:200), TWIST (ab50581, Abcam, 1:100), YFP (ab13970, Abcam, 1:1000), ZEB1 (NBP1-05987, Novus, 1:500), and ZEB2 (NBP1-82991, Novus, 1:100). Sections for pimonidazole adduct (HPI Inc., 1:50) or αSMA immunohistochemistry staining were blocked with M.O.M kit (Vector Laboratories, West Grove, PA) and developed by DAB according to the manufacturer's recommendations. Alternatively, for immunofluorescence, sections were dual-labeled using secondary antibodies conjugated to Alexa fluor-488 or -594 or tyramide signal amplification (TSA, PerkinElmer) conjugated to FITC. Lineage traced (YFP positive) EMT analysis was performed on 8 μm thick O.C.T. medium (TissueTek) embedded frozen sections. Sections were stained for αSMA (ab5694, Abcam, 1:400) followed by Alexa fluor-680 conjugated secondary antibody. Bright field imagery was obtained on a Leica DM1000 light microscope or the Perkin Elmer 3DHistotech Slide Scanner. Fluorescence imagery was obtained on a Zeiss Axio Imager.M2 or the Perkin Elmer Vectra Multispectral imaging platform. The images were quantified for percent positive area using NIH ImageJ analysis software (αSMA, Pimonidazole, SLUG, and CD31), percent positive cells using InForm analysis software (Ki-67 and CD3), or scored for intensity either positive or negative (CK19, YFP, ZEB1, ZEB2, SOX4, and Cleaved Caspase-3) or on a scale of 1-3 (E-cadherin) or 1-4 (ENT1, ENT2 and CNT3).

In situ hybridization

In situ hybridization (ISH) was performed on frozen tumor sections as previously described[34]. In brief, 10 μm-thick sections were hybridized with antisense probes to *Twist1* and *Snai1* overnight at 65°C. After hybridization, sections were washed and incubated with AP-conjugated sheep anti-DIG antibody (1:2000; Roche) for 90 min at room temperature. After three washes, sections were incubated in BM Purple (Roche) until positive staining was seen. Digoxigenin labeled *in situ* riboprobes were generated by *in vitro* transcription method (Promega and Roche) using a PCR template. The following primers were used to generate the template PCR product. *Twist1*; forward (5'-CGGCCAGGTACATCGACTTC-3') and reverse (5'-TAATACGACTCACTATAGGGAGATTTAAAAGTGTGCCCCACGC-3') *Snai1*: forward (5'-CAACCGTGCTTTTGCTGAC-3') and reverse (5'-TAATACGACTCACTATAGGGAGACCTTTAAAATGTAAACATCTTTCTCC-3')

Gene Expression Profiling

Total RNA was isolated from tumors of KPC control, KPC; Twist[cKO] and KPC; Snail[cKO] mice (n = 3 in each group) by TRIzol (15596026, Life Technologies) and submitted to the Microarray Core Facility at MD Anderson Cancer Center. Gene expression analysis was performed using Mouse Ref6 Gene Expression Bead Chip (Illumina). The Limma package from R Bioconductor[35] was used for quantile normalization of expression arrays and to analyze differentially expressed genes between cKO and control sample groups (p ≤ 0.05 and fold change ≥ 1.2). Gene expression microarray data was deposited in GEO (Accession number GSE66981). Genes up-regulated in cells acquiring an EMT program were expected to be down-regulated in the Twist[cKO] and Snail[cKO] tumors compared to control tumors.

CTC assays

Blood (200 μL) was collected from KPC;LSL-YFP and KPC; Twist[cKO];LSL-YFP (ROSA-LSL-YFP lineage tracing of cancer cells) mice and incubated with 10 ml of ACK lysis buffer (A1049201, Gibco) at room temperature to lyse red blood cells. Cell pellets were resuspended in 2% FBS containing PBS and analyzed for the number of YFP$^+$ cells by flow cytometry (BD LSRFortessa X-20 Cell Analyzer). The data was expressed as the percent YFP$^+$ cells from gated cells, with 100,000 cells analyzed at the time of acquisition. Whole blood cell pellets were also assayed for the expression of *Kras^{G12D}* transcripts, using quantitative real-time PCR analyses (described below).

Primary pancreatic adenocarcinoma cell culture and analyses

Derivation of primary PDAC cell lines were performed as previously described[36]. Fresh tumors were minced with sterile razor blades, digested with dispase II (17105041, Gibco, 4 mg/ml)/collagenase IV (17104019, Gibco, 4 mg/ml)/RPMI for 1 h at 37°C, filtered by a 70 μm cell strainer, resuspended in RPMI/20%FBS and then seeded on collagen I coated plates (087747, Fisher Scientific). Cells were maintained in RPMI medium with 20% FBS and 1% penicillin, streptomycin and amphotericin B (PSA) antibiotic mixture. Cancer cells were further purified by FACS based on YFP or E-Cadherin expression (anti-E-cadherin antibody, 50-3249-82, eBioscience, 1:100). The sorted cells, using BD FACSAria™ II sorter (South

Campus Flow Cytometry Core Lab of MD Anderson Cancer Center) were subsequently expanded *in vitro*. All studies were performed on cells cultivated less than 30 passages. As these are primary cell lines no further authentication methods were applicable and no mycoplasma tests were performed.

MTT and drug sensitivity assays

MTT assay was performed to detect cell proliferation and viability by using Thiazolyl Blue Tetrazolium Bromide (MTT, M2128, Sigma) following the manufacturer's recommendations with an incubation of two hours at 37°C. For the drug treatment studies, a cell line derived from each of the KPC, KPC; Snail^{cKO} and KPC; Twist^{cKO} mice was treated with 20 μM Gemcitabine (G-4177, LC Laboratories) or 100 μM erlotinib (5083S, NEB) for 48 hours. The relative cell viability was detected using MTT assay with a cell line derived from each of the KPC, KPC; Snail^{cKO} and KPC; Twist^{cKO} mice. N value is defined as biological replicates of a single cell line. Control conditions included 1% DMSO vehicle for erlotinib. The relative absorbance was normalized and control (time 0 hour or vehicle treated) arbitrarily set to 1 or 100% for absorbance or drug survival, respectively.

Quantitative real-time PCR analyses (qPCR)

RNA was extracted from whole blood cell pellets following ACK lysis using the PicoPure Extraction kit as directed (KIT0214, Arcturus), or from cultured primary pancreatic adenocarcinoma cells using TRIzol (15596026, Life Technologies). cDNA was synthetized using TaqMan Reverse Transcription Reagents (N8080234, Applied Biosystems) or High Capacity cDNA Reverse Transcription Kit (4368814, Applied Biosystems). Primers for *Kras^{G12D}* recombination are: *Kras^{G12D}* forward (5' ACTTGTGGTGGTTGGAGCAGC 3'), *Kras^{G12D}* reverse (5' TAGGGTCATACTCATCCACAA 3'). 1/ Ct values are presented to show *Kras^{G12D}* expression in indicated experimental groups, statistical analyses were assayed on Ct. Primer sequences for EMT related genes are listed in Supplemental Table 1, GAPDH was used as an internal control. The data is presented as the relative fold change and statistical analyses were assayed on Ct.

Tumor sphere assay

Tumor sphere assays were performed as previously described[33]. Two million cultured primary tumor cells were plated in a low-adherence 100mm dish (FB0875713, Fisherbrand) with 1% fetal bovine serum, Dulbecco's modified Eagle's medium, and penicillin/streptomycin/amphotericin. Cells were incubated for seven days and formed spheres were counted at 100x magnification. Three, two and three cell lines were analyzed for KPC control, KPC; Twist^{cKO} and KPC; Snail^{cKO} group, respectively, five field of views per cell line were quantified.

MRI Analyses

MRI imaging was performed using a 7T small animal MR system as previously described[37]. To measure tumor volume, suspected regions were drawn blinded on each slice based on normalized intensities. The volume was calculated by the addition of delineated regions of interest in $mm^2 \times 1$ mm slice distance. None of the mice had a tumor burden that exceeded

1.5 cm in diameter, in accordance with institutional regulations. All mice with measurable tumors were enrolled in the study (see **Extended Table 3**). Mice were imaged twice, once at the beginning of the enrollment (Day 0), and a second time 20 days (Day 19) afterwards. Surviving animals were euthanized at end point (Day 21) for histological characterization.

Statistical analyses

Statistical analyses were performed on the mean values of biological replicates in each group using unpaired two-tailed or one-tailed t-tests (qPCR only), one-way ANOVA with Tukey's multiple comparisons test using GraphPad Prism, as stipulated in the figure legends. χ^2 analyses, using SPSS statistical software, were performed comparing control to cKO groups for metastatic or colonization frequency across multiple histological parameters in all mice and mice 120 days of age. Fisher's Exact P value was used to determine significance. Results are outlined in **Extended Table 2**. Kaplan-Meier plots were drawn for survival analysis and the log rank Mantel-Cox test was used to evaluate statistical differences, using GraphPad Prism. Data met the assumptions of each statistical test, where variance was not equal (determined by an F-test) Welch's correction for unequal variances was applied. Error bars represent s.e.m. when multiple visual fields were averaged to produce a single value for each animal which was then averaged again to represent the mean bar for the group in each graph. $P < 0.05$ was considered statistically significant.

Extended Data
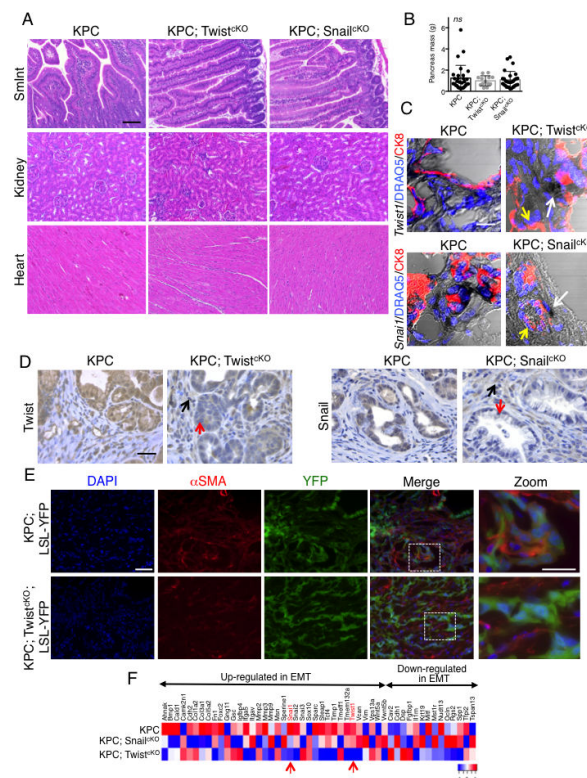
Extended Figure 1.

A Representative H&E images of small intestine (SmInt), kidney, and heart (scale, 100μm). **B** Pancreatic mass of (n = 29, 13, and n = 28 mice; s.d.; one-way ANOVA). **C** Merge of *Twist1* or *Snai1 in situ* hybridization (black) followed by CK8 (red) immunolabeling in tumors from KPC and KPC; Twist^cKO or KPC; Snail^cKO mice, respectively. White arrows highlight positive cells in the stroma while yellow arrows highlight negative epithelium (scale, 50 μm). **D** Twist or Snail immunostaining in KPC and KPC; Twist^cKO or KPC; Snail^cKO tumors, respectively. Black arrows highlight positive cells in the stroma while red arrows highlight negative epithelium (scale, 20 μm). **E** Channel separations of the representative images of αSMA immunolabeling in YFP lineage traced tumors found in **Figure 1F** (scale, 50 μm). **F** EMT gene expression signature analysis in KPC, KPC; Twist^cKO and KPC; Snail^cKO cohorts (n = 3 mice). Red arrows indicate reduced *Twist1* and *Snai1* expression in KPC; Twist^cKO and KPC; Snail^cKO cohorts, respectively.
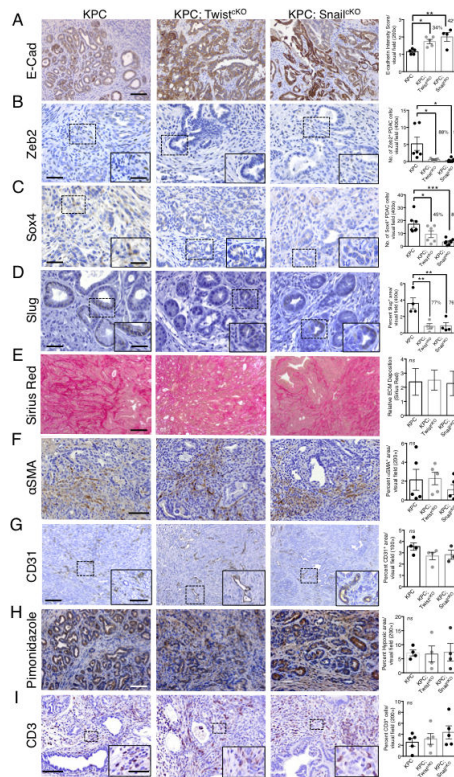
Extended Figure 2.
A E-Cadherin immunolabeling and quantification of primary KPC (n = 5 mice), KPC; Twist^cKO (n = 5 mice) and KPC; Snail^cKO (n = 4 mice) (scale, 100 μm). **B** Zeb2 immunolabeling and quantification of primary KPC (n = 6 mice), KPC; Twist^cKO (n = 5 mice) and KPC; Snail^cKO (n = 7 mice) (scale, 50 μm; inset scale, 20 μm). **C** Sox4 immunolabeling and quantification of primary KPC (n = 7 mice), KPC; Twist^cKO (n = 6 mice) and KPC; Snail^cKO (n = 8 mice) (scale, 50 μm; inset scale, 20 μm). **D** Slug immunolabeling and quantification of primary KPC (n = 4 mice), KPC; Twist^cKO (n = 4 mice) and KPC; Snail^cKO (n = 4 mice) tumors (scale, 50 μm; inset scale, 20 μm). **E** Sirius Red staining and quantification of primary KPC (n = 21 mice), KPC;Twist^cKO (n = 8 mice) and KPC;Snail^cKO (n = 11 mice) (scale, 200 μm; s.d.) **F** αSMA immunolabeling and

quantification of primary KPC (n = 5 mice), KPC;Twist^cKO (n = 5 mice) and KPC;Snail^cKO (n = 5 mice) (scale, 100 μm). **G** CD31 immunolabeling and quantification of primary KPC (n = 4 mice), KPC;Twist^cKO (n = 4 mice) and KPC;Snail^cKO (n = 3 mice) (scale, 200 μm, inset scale, 100 μm). **H** Pimonidazole staining and quantification of primary KPC (n = 4 mice), KPC; Twist^cKO (n = 4 mice) and KPC; Snail^cKO (n = 4 mice) (scale, 100 μm). **I** CD3 immunolabeling and quantification of primary KPC (n = 5 mice), KPC;Twist^cKO (n = 5 mice) and KPC;Snail^cKO (n = 5 mice) (scale, 100 μm; inset scale, 25 μm). Unless otherwise indicated error bars represent s.e.m, and significance determined by One-way ANOVA. *P< 0.05, ** P<0.01, *** P<0.001. *ns*, not significant.
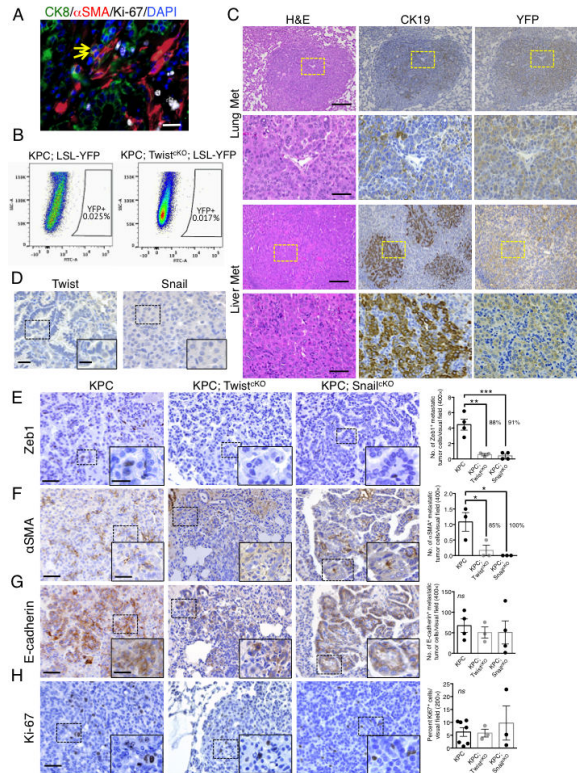
Extended Figure 3.
A Immunolabeling of primary tumors (n = 3 mice) for αSMA (red), CK8 (green), Ki-67 (white) and DAPI (blue); yellow arrows point to EMT^+ cells (scale, 20 μm). **B** Representative dot plots of circulating YFP^+ cells. **C** Images of serial sections of KPC; LSL-YFP lung and liver metastasis stained for H&E or immunolabeled for CK19 or YFP. Yellow dashed box represents magnified areas in panel below (scale, 200 μm; magnification scale, 100 μm). **D** KPC metastatic tumors stained for Twist and Snail (n = 3 mice; scale, 50 μm; inset scale, 20 μm). **E** Zeb1 immunolabeling and quantification of metastatic KPC (n = 4 mice), KPC; Twist^cKO (n = 3 mice) and KPC; Snail^cKO (n = 4 mice) (scale, 50 μm; inset scale, 20 μm). **F** αSMA immunolabeling and quantification of metastatic KPC (n = 3 mice), KPC; Twist^cKO (n = 3 mice) and KPC; Snail^cKO (n = 3 mice) (scale, 50 μm; inset scale, 20 μm). **G** E-Cadherin staining on serial sections of αSMA immunolabeling and quantification of metastatic KPC (n = 4 mice), KPC; Twist^cKO (n = 3 mice) and KPC; Snail^cKO (n = 4 mice) (scale, 50 μm; inset scale, 20 μm). **H** Ki-67 immunolabeling and quantification of

metastatic KPC (n = 7 mice), KPC; Twist[cKO] (n = 3 mice) and KPC; Snail[cKO] (n = 3 mice) (scale, 50 μm). Unless otherwise indicated error bars represent s.e.m, percentages indicated represent percent decrease from control, and significance determined by One-way ANOVA. * P<0.05, ** P<0.01, *** P<0.001. ns, not significant.
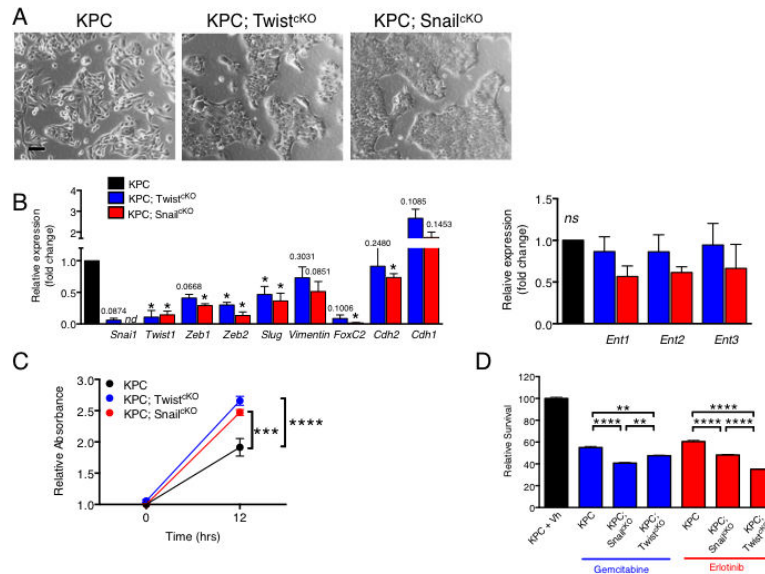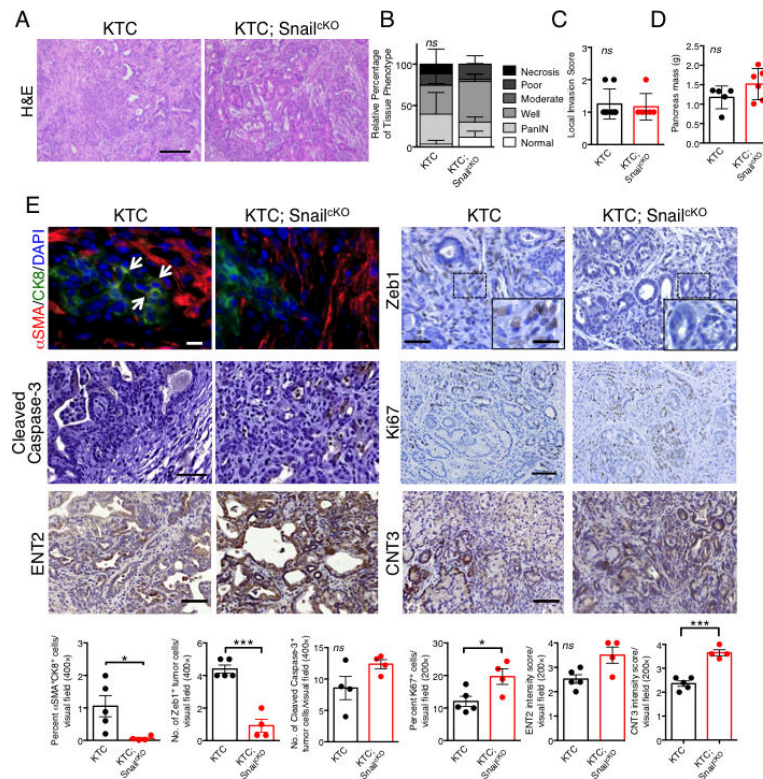

Extended Figure 4.
A Brightfield micrograph of cultured primary KPC, KPC; Twist[cKO] and KPC; Snail[cKO] cells (scale, 50 μm). **B** EMT and gemcitabine transport related gene expression shown by qPCR analysis in KPC (n = 3-4 cell lines), KPC; Twist[cKO] (n = 5 cell lines) and KPC; Snail[cKO] (n = 5-6 cell lines) (s.d., one-tailed t-test, * P< 0.05, numbers list non-significant P values. nd: not detected, ns: not significant). **C** MTT assay showing cell proliferation in KPC, KPC; Twist[cKO] and KPC; Snail[cKO] cells (n = 8, 8, and 8 biological replicates of a cell line for each genotype). **D** Relative cell viability (MTT assay) in cultured KPC, KPC; Twist[cKO] and KPC; Snail[cKO] cells treated with gemcitabine or erlotinib (n = 8, 8, and 8 biological replicates of a cell line for each genotype). Unless otherwise indicated error bars represent s.e.m, significance was determined by one-way ANOVA. ** P<0.01, *** P<0.001, **** P <0.0001.

Extended Figure 5.

A Representative H&E images (scale, 100 μm). **B** Relative percentage of each histological tissue phenotype of KTC (n = 8 mice) and KTC; Snail[cKO] (n = 6 mice) primary tumors (s.d.). **C** Primary tumor invasiveness in KTC (n = 8 mice) and KTC; Snail[cKO] (n = 6 mice) (s.d.). **D** Pancreatic mass in KTC (n = 5 mice) and KTC; Snail[cKO] (n = 6 mice) (s.d.). **E** Immunolabeling and quantification of primary KTC (n = 5 mice), KTC; Snail[cKO] (n = 4 mice) for αSMA (red), CK8 (green) and DAPI (blue); white arrows indicate double positive cells (scale, 20 μm), Zeb1 (scale, 50 μm; inset scale. 20μm), cleaved caspase-3 (scale, 50 μm; n = 4 and 4 mice), Ki-67 (scale, 100 μm), ENT2 (scale, 100 μm) and CNT3 (scale, 100 μm). Unless otherwise indicated error bars represent s.e.m, and significance determined by two-tailed t-test. * *P*<0.05, *** *P*<0.001. ns, not significant.
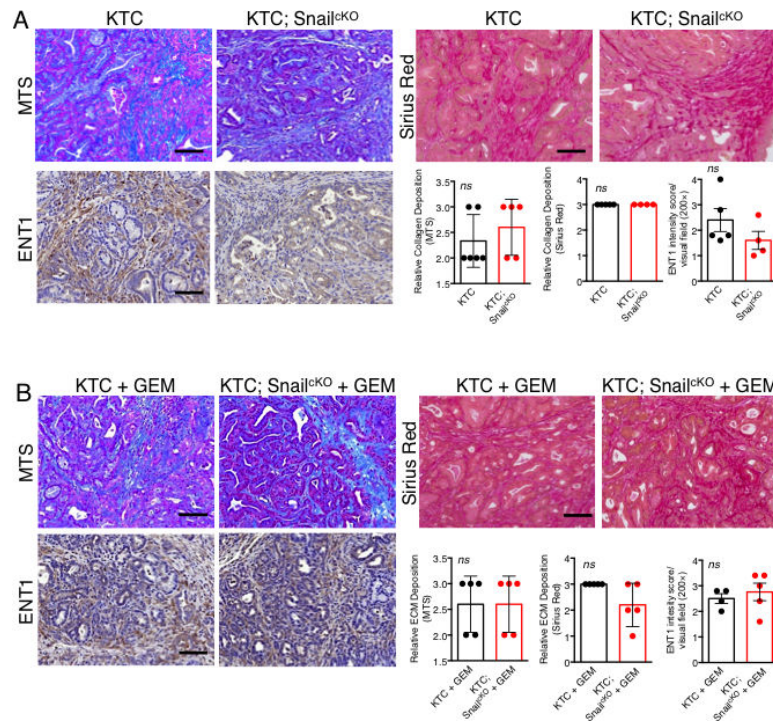
Extended Figure 6.
A-B Staining and quantification of (**A**) KTC (n = 5 or 6 mice), KTC; Snail^cKO (n = 4 or 5 mice) (**B**) KTC + GEM (n = 4 or 5 mice), KTC; Snail^cKO + GEM (n = 5 mice) for Masson's Trichrome Stain (MTS) (scale, 200 μm), Sirius Red staining (scale, 200 μm), and ENT1 (scale, 100 μm). Error bars represent s.d. (MTS and Sirius Red) or s.e.m. (ENT1), and significance determined by two-tailed t-test. ns, not significant.

Extended Table 1

Pathological spectrum of disease and metastasis in KPC, KPC; Twist^cKO and KPC; Snail^cKO cohorts.

Pathological Spectrum within cohorts

ID	AGE	PDA	Differentiation	Histology 1	Histology 2	Liver	Lung	Spleen	Any	Moribund
KPC	**(104)**									
1	158	Y	W	S	G	Y	Y	N	Y	Y
2	165	Y	W	G		N	N	N	N	Y
3	148	Y	P	S	G	N	N	-	N	Y
4	135	Y	M	S	G	Y	N	Y	Y	Y
5	95	Y	M	G		N	Y	N	Y	N
6	42	Y	M	G		N	N	N	N	Y
7	55	Y	P	G	S	Y	N	N	Y	Y
8	91	Y	M	G		N	N	N	N	N
9	87	Y	W	G		N	N	N	N	N
10	63	Y	P	G		Y	Y	Y	Y	N
11	108	Y	P	S	G	Y	N	N	Y	FD
12	110	Y	W	G		N	N	N	N	N
13	104	Y	W	G		Y	N	N	Y	Y
14	54	Y	W	S	G	N	N	N	N	Y
15	108	Y	P	S	G	N	Y	N	Y	Y
16	42	Y	P	S	G	N	N	N	N	Y
17	68	Y	W	G		N	N	N	N	N
18	107	Y	P	G		N	N	N	N	N
19	87	Y	P	G		N	N	N	N	N
20	48	Y	P	G	S	N	N	N	N	Y
21	109	Y	P	G	S	Y	Y	N	Y	FD
22	81	Y	P	G		Y	Y	N	Y	Y
23	151	Y	W	G		N	Y	N	Y	Y
24	47	Y	M	G	S	N	Y	N	Y	Y
25	143	Y	P	G	S	N	Y	N	Y	Y
26	122	Y	W	G		Y	N	N	Y	N

Pathological Spectrum within cohorts

ID	AGE	PDA	Differentiation	Histology 1	Histology 2	Liver	Lung	Spleen	Any	Moribund
27	115	Y	P	G		Y	Y	N	Y	N
28	76	Y	W	G		N	Y	N	Y	N
29	122	Y	M	S	G	Y	N	N	Y	Y
30	97	Y	P	G		N	N	N	N	N
31	107	Y	W	G		N	N	N	N	N
Totals	(Median)	31/31				11/31	11/31	2/30	17/31	
%		100.0%				35.5%	35.5%	6.7%	54.8%	
Twist^eKO	**(111)**									
1	148	Y	W	G	S	Y	N	N	Y	N
2	151	Y	P	S	G	Y	Y	Y	Y	N
3	140	Y	P	G		Y	Y	N	Y	Y
4	53	Y	P	G	S	N	N	N	N	Y
5	43	Y	P	G		N	N	N	N	Y
6	117	Y	P	G	S	N	N	N	Y	N
7	90	Y	P	S	G	Y	N	N	Y	Y
8	52	Y	P	G	S	N	N	N	N	Y
9	104	Y	P	G		N	N	N	N	N
10	218	Y	P	G	S	N	N	Y	Y	Y
11	153	Y	P	G		N	Y	N	Y	Y
12	45	Y	P	G	S	N	N	N	N	Y
13	77	Y	P	G	S	Y	N	N	Y	Y
14	126	Y	P	G	S	Y	Y	N	Y	Y
Totals	(Median)	14/14				6/14	4/14	2/14	8/14	
%		100.0%				42.9%	28.6%	14.3%	57.1%	
Snail^eKO	**(103)**									
1	144	Y	W	G		N	Y	N	Y	N
2	51	Y	P	G	S	N	N	N	N	Y

Pathological Spectrum within cohorts

ID	AGE	PDA	Differentiation	Histology 1	Histology 2	Liver	Lung	Spleen	Any	Moribund
3	105	Y	P	G	S	N	Y	N	Y	Y
4	111	Y	P	G		N	N	N	N	N
5	106	Y	P	G	S	Y	N	Y	Y	Y
6	129	Y	P	G		N	N	N	N	N
7	102	Y	P	G	S	N	Y	-	Y	N
8	98	Y	P	G	S	Y	N	Y	Y	N
9	47	Y	P	G	S	N	N	N	N	Y
10	54	Y	W	G		Y	Y	N	Y	FD
11	59	Y	M	G		Y	N	N	Y	N
12	103	Y	P	G		Y	N	N	Y	N
13	60	Y	P	S	G	Y	N	Y	Y	Y
14	77	Y	P	G		Y	N	N	Y	Y
15	57	Y	M	S	G	Y	N	N	Y	FD
16	130	Y	P	G		Y	Y	N	Y	FD
17	76	Y	P	G	S	N	N	N	N	FD
18	111	Y	P	G		N	Y	N	Y	Y
19	100	Y	P	G	S	Y	N	Y	Y	FD
20	104	Y	P	G	S	Y	N	N	Y	Y
21	124	Y	M	G		N	N	N	N	FD
22	88	Y	P	G	S	N	N	N	Y	Y
23	192	Y	W	G		Y	Y	N	Y	Y
24	122	Y	P	G		N	N	N	N	Y
25	60	Y	W	G	S	N	N	N	N	Y
26	112	Y	W	G		N	Y	N	Y	N
27	48	Y	P	G	S	N	N	N	N	Y
28	48	Y	P	G	S	N	Y	N	Y	Y
29	124	Y	P	G	S	Y	Y	Y	Y	N
30	215	Y	W	G		N	N	N	N	N
Totals	(Median)	30/30				13/30	9/30	5/29	18/30	
%		100.0%				43.3%	30.0%	17.2%	60.0%	

Key: (Y) yes. (N) no, (W) well, (M) moderate, (P) poor, (G) glandular, (S) sarcomatoid, (FD) found dead, (–) no tissue

Extended Table 2

Results of χ^2 analysis reporting Fisher's Exact P value.

$\chi 2$ **Analysis**		
Group	**Perameter**	**Fisher's Exact P value**
Differentiation	**All Ages**	
Control vs. Twist[cKO]	Early Tumor progression	0.458
Control vs. Snail[cKO]		0.106
Control vs. Twist[cKO]	Late Tumor progression	0.458
Control vs. Snail[cKO]		0.106
Control vs. Twist[cKO]	Sarcomatoid	0.108
Control vs. Snail[cKO]		0.446
Differentiation	**120 days**	
Control vs. Twist[cKO]	Early Tumor progression	0.580

χ2 Analysis		
Group	**Perameter**	**Fisher's Exact *P* value**
Control vs. Snail[cKO]		0.569
Control vs. Twist[cKO]	Late Tumor progression	0.580
Control vs. Snail[cKO]		0.569
Control vs. Twist[cKO]	Sarcomatoid	1.000
Control vs. Snail[cKO]		0.119
Metastasis	**All Ages**	
Control vs. Twist[cKO]	Liver Metastasis	0.744
Control vs. Snail[cKO]		0.358
Control vs. Twist[cKO]	Lung Metastasis	0.743
Control vs. Snail[cKO]		0.786
Control vs. Twist[cKO]	Spleen Invasion	0.581
Control vs. Snail[cKO]		0.254
Control vs. Twist[cKO]	Any Metastasis	1.000
Control vs. Snail[cKO]		0.797
Metastasis	**120 days**	
Control vs. Twist[cKO]	Liver Metastasis	0.627
Control vs. SnailcKO		1.000
Control vs. Twist[cKO]	Lung Metastasis	0.592
Control vs. SnailcKO		1.000
Control vs. Twist[cKO]	Spleen Invasion	0.559
Control vs. SnailcKO		1.000
Control vs. Twist[cKO]	Any Metastasis	0.473
Control vs. SnailcKO		0.608

Extended Table 3

Pathological spectrum of disease and metastasis in KPC, KPC; Twist[cKO] and KPC; Snail[cKO] cohorts treated with Gemcitabine

KPC Gemcitabine cohorts				
ID	**Start Age (Days)**	**Start Volume (mm³)**	**End Volume (mm³)**	**Survival (Days)**
KPC + GEM	**(89)**			**(13)**
1	148	1610.351	D	7
2	72	29.736	D	13
3	72	439.795	902.759	21

KPC Gemcitabine cohorts

ID	Start Age (Days)	Start Volume (mm³)	End Volume (mm³)	Survival (Days)
4	80	44.14	D	14
5	100	536.304	592.31	21
6	89	166.968	D	2
7	94	52.734	D	7
6	122	90.211	D	14
9	164	217.919	D	8
10	143	212.817	D	18
11	84	323.829	897.217	21
12	58	76.734	D	4
13	58	116.186	D	8
Mean	(Median)	301.4	797.4	
Stdev		406.9	145.1	
Twist^cKO + GEM	**(79)**			**(21)**
1	117	243.0	644.2	21
2	75	47.2	180.0	21
3	75	45.4	460.9	21
4	78	54.6	47.5	21
5	46	53.7	66.5	21
6	96	63.1	D	13
7	90	23.9	D	13
8	79	101.0	D	14
9	52	28.5	D	14
10	52	49.4	98.706	21
11	104	43.4	127.0	21
12	104	53.5	12.1	21
13	68	56.7	D	15
14	122	650.1	164.1	21
15	104	181.8	78.6	21
Mean	(Median)	113.0	187.9	
Stdev		154.8	193.0	
Snail^cKO + GEM	**(96)**			**(21)**
1	188	255.2	D	12
2	181	854.7	D	4
3	127	32.0	59.6	21
4	127	58.7	107.4	21
5	142	109.8	D	14
6	54	33.6	57.2	21
7	89	17.0	D	13

KPC Gemcitabine cohorts

ID	Start Age (Days)	Start Volume (mm³)	End Volume (mm³)	Survival (Days)
8	78	54.9	39.6	21
9	78	3.1	D	15
10	104	209.7	134.3	21
11	96	220.0	280.2	21
12	96	24.1	46.2	21
13	119	711.0	D	18
14	126	655.6	805.4	21
15	119	168.6	D	18
16	82	453.8	517.4	21
17	82	56.7	74.1	21
18	90	40.0	D	16
19	67	80.5	D	10
20	66	49.5	226.2	21
Mean	(Median)	204.4	213.4	
Stdev		250.7	231.7	

Key: (D) died

Supplementary Material

Refer to Web version on PubMed Central for supplementary material.

Acknowledgements

References

1. Hotz B, et al. Epithelial to mesenchymal transition: expression of the regulators snail, slug, and twist in pancreatic cancer. Clinical cancer research : an official journal of the American Association for Cancer Research. 2007; 13:4769–4776. doi:10.1158/1078-0432.CCR-06-2926. [PubMed: 17699854]

2. Arumugam T, et al. Epithelial to mesenchymal transition contributes to drug resistance in pancreatic cancer. Cancer research. 2009; 69:5820–5828. doi:10.1158/0008-5472.CAN-08-2819. [PubMed: 19584296]

3. Taube JH, et al. Core epithelial-to-mesenchymal transition interactome gene- expression signature is associated with claudin-low and metaplastic breast cancer subtypes. Proceedings of the National Academy of Sciences of the United States of America. 2010; 107:15449–15454. doi:10.1073/pnas.1004900107. [PubMed: 20713713]

4. Rhim AD, et al. EMT and dissemination precede pancreatic tumor formation. Cell. 2012; 148:349–361. doi:10.1016/j.cell.2011.11.025. [PubMed: 22265420]

5. Kalluri R, Weinberg RA. The basics of epithelial-mesenchymal transition. The Journal of clinical investigation. 2009; 119:1420–1428. doi:10.1172/jci39104. [PubMed: 19487818]

6. McDonald OG, Maitra A, Hruban RH. Human correlates of provocative questions in pancreatic pathology. Advances in anatomic pathology. 2012; 19:351–362. doi:10.1097/PAP. 0b013e318273f998. [PubMed: 23060061]

7. Guaita S, et al. Snail induction of epithelial to mesenchymal transition in tumor cells is accompanied by MUC1 repression and ZEB1 expression. The Journal of biological chemistry. 2002; 277:39209–39216. doi:10.1074/jbc.M206400200. [PubMed: 12161443]

8. Wellner U, et al. The EMT-activator ZEB1 promotes tumorigenicity by repressing stemness-inhibiting microRNAs. Nature cell biology. 2009; 11:1487–1495. doi:10.1038/ncb1998. [PubMed: 19935649]

9. Zhang K, et al. Knockdown of snail sensitizes pancreatic cancer cells to chemotherapeutic agents and irradiation. International journal of molecular sciences. 2010; 11:4891–4892. doi:10.3390/ijms11124891. [PubMed: 21614180]

10. Tsai JH, Donaher JL, Murphy DA, Chau S, Yang J. Spatiotemporal regulation of epithelial-mesenchymal transition is essential for squamous cell carcinoma metastasis. Cancer cell. 2012; 22:725–736. doi:10.1016/j.ccr.2012.09.022. [PubMed: 23201165]

11. Stockinger A, Eger A, Wolf J, Beug H, Foisner R. E-cadherin regulates cell growth by modulating proliferation-dependent beta-catenin transcriptional activity. The Journal of cell biology. 2001; 154:1185–1196. doi:10.1083/jcb.200104036. [PubMed: 11564756]

12. Muraoka-Cook RS, Dumont N, Arteaga CL. Dual role of transforming growth factor beta in mammary tumorigenesis and metastatic progression. Clinical cancer research : an official journal of the American Association for Cancer Research. 2005; 11:937s–943s. [PubMed: 15701890]

13. Hugo HJ, et al. Direct repression of MYB by ZEB1 suppresses proliferation and epithelial gene expression during epithelial-to-mesenchymal transition of breast cancer cells. Breast cancer research : BCR. 2013; 15:R113. doi:10.1186/bcr3580. [PubMed: 24283570]

14. Mani SA, et al. The epithelial-mesenchymal transition generates cells with properties of stem cells. Cell. 2008; 133:704–715. doi:10.1016/j.cell.2008.03.027. [PubMed: 18485877]

15. Liu H, et al. Cancer stem cells from human breast tumors are involved in spontaneous metastases in orthotopic mouse models. Proceedings of the National Academy of Sciences of the United States of America. 2010; 107:18115–18120. doi:10.1073/pnas.1006732107. [PubMed: 20921380]

16. Wang Z, et al. Activated K-Ras and INK4a/Arf deficiency promote aggressiveness of pancreatic cancer by induction of EMT consistent with cancer stem cell phenotype. Journal of cellular physiology. 2013; 228:556–562. doi:10.1002/jcp.24162. [PubMed: 22806240]

17. Yang J, et al. Twist, a master regulator of morphogenesis, plays an essential role in tumor metastasis. Cell. 2004; 117:927–939. doi:10.1016/j.cell.2004.06.006. [PubMed: 15210113]

18. Vega S, et al. Snail blocks the cell cycle and confers resistance to cell death. Genes & development. 2004; 18:1131–1143. doi:10.1101/gad.294104. [PubMed: 15155580]

19. Shah AN, et al. Development and characterization of gemcitabine-resistant pancreatic tumor cells. Annals of surgical oncology. 2007; 14:3629–3637. doi:10.1245/s10434-007-9583-5. [PubMed: 17909916]

20. Yin T, et al. Expression of snail in pancreatic cancer promotes metastasis and chemoresistance. The Journal of surgical research. 2007; 141:196–203. doi:10.1016/j.jss.2006.09.027. [PubMed: 17583745]

21. Wang Z, et al. Acquisition of epithelial-mesenchymal transition phenotype of gemcitabine-resistant pancreatic cancer cells is linked with activation of the notch signaling pathway. Cancer research. 2009; 69:2400–2407. doi:10.1158/0008-5472.CAN-08-4312. [PubMed: 19276344]

22. Alagesan B, et al. Combined MEK and PI3K inhibition in a mouse model of pancreatic cancer. Clinical cancer research : an official journal of the American Association for Cancer Research. 2015; 21:396–404. doi:10.1158/1078-0432.ccr-14-1591. [PubMed: 25348516]

23. Cursons J, et al. Stimulus-dependent differences in signalling regulate epithelial mesenchymal plasticity and change the effects of drugs in breast cancer cell lines. Cell communication and signaling : CCS. 2015; 13:26. doi:10.1186/s12964-015-0106-x. [PubMed: 25975820]

24. Javle MM, et al. Epithelial-mesenchymal transition (EMT) and activated extracellular signal-regulated kinase (p-Erk) in surgically resected pancreatic cancer. Annals of surgical oncology. 2007; 14:3527–3533. doi:10.1245/s10434-007-9540-3. [PubMed: 17879119]

25. Masugi Y, et al. Solitary cell infiltration is a novel indicator of poor prognosis and epithelial-mesenchymal transition in pancreatic cancer. Human pathology. 2010; 41:1061–1068. doi: 10.1016/j.humpath.2010.01.016. [PubMed: 20413143]

26. Park JY, et al. Pdx1 expression in pancreatic precursor lesions and neoplasms. Applied immunohistochemistry & molecular morphology : AIMM / official publication of the Society for Applied Immunohistochemistry. 2011; 19:444–449. doi:10.1097/PAI.0b013e318206d958. [PubMed: 21297446]

27. Offield MF, et al. PDX-1 is required for pancreatic outgrowth and differentiation of the rostral duodenum. Development. 1996; 122:983–995. [PubMed: 8631275]

28. Hidalgo M. Pancreatic cancer. The New England journal of medicine. 2010; 362:1605–1617. doi: 10.1056/NEJMra0901557. [PubMed: 20427809]

29. Kleger A, Perkhofer L, Seufferlein T. Smarter drugs emerging in pancreatic cancer therapy. Annals of oncology : official journal of the European Society for Medical Oncology / ESMO. 2014; 25:1260–1270. doi:10.1093/annonc/mdu013. [PubMed: 24631947]

30. Gore AJ, Deitz SL, Palam LR, Craven KE, Korc M. Pancreatic cancer-associated retinoblastoma 1 dysfunction enables TGF-beta to promote proliferation. The Journal of clinical investigation. 2014; 124:338–352. doi:10.1172/jci71526. [PubMed: 24334458]

31. Hingorani SR, et al. Trp53R172H and KrasG12D cooperate to promote chromosomal instability and widely metastatic pancreatic ductal adenocarcinoma in mice. Cancer cell. 2005; 7:469–483. doi:10.1016/j.ccr.2005.04.023. [PubMed: 15894267]

32. Ijichi H, et al. Aggressive pancreatic ductal adenocarcinoma in mice caused by pancreas-specific blockade of transforming growth factor-beta signaling in cooperation with active Kras expression. Genes & development. 2006; 20:3147–3160. doi:10.1101/gad.1475506. [PubMed: 17114585]

33. Ozdemir BC, et al. Depletion of carcinoma-associated fibroblasts and fibrosis induces immunosuppression and accelerates pancreas cancer with reduced survival. Cancer cell. 2014; 25:719–734. doi:10.1016/j.ccr.2014.04.005. [PubMed: 24856586]

34. Keskin D, et al. Targeting Vascular Pericytes in Hypoxic Tumors Increases Lung Metastasis via Angiopoietin-2. Cell reports. 2015; 10:1066–1081. doi:10.1016/j.celrep.2015.01.035. [PubMed: 25704811]

35. Smyth, GK. Limma: linear models for microarray data. In Bioinformatics and Computational Biology Solutions using R and Bioconductor. Gentleman, R.; Carey, V.; Dudoit, S.; Irizarry, R.; Huber, W., editors. Springer; New York: 2005.

36. Ying H, et al. Oncogenic Kras maintains pancreatic tumors through regulation of anabolic glucose metabolism. Cell. 2012; 149:656–670. doi:10.1016/j.cell.2012.01.058. [PubMed: 22541435]

37. Melo SA, et al. Glypican-1 identifies cancer exosomes and detects early pancreatic cancer. Nature. 2015; 523:177–182. doi:10.1038/nature14581. [PubMed: 26106858]
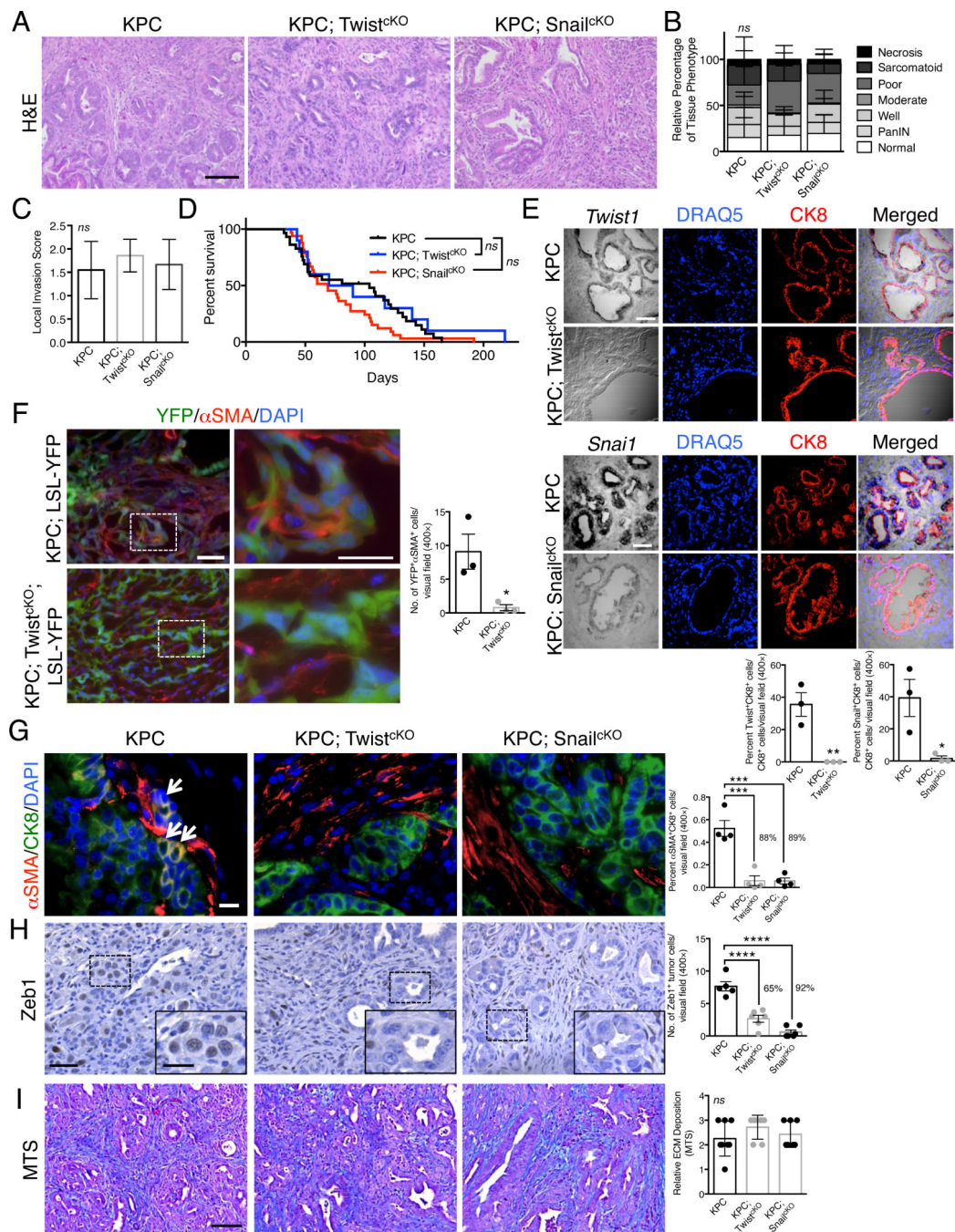
Figure 1. EMT inhibition does not alter primary tumor progression
A Representative H&E stained primary tumors (scale; 100μm). **B** Relative percentages of each primary tumor histological tissue phenotype (n = 31, 14, and 30 mice; s.d.). **C** Local invasiveness (n = 31, 14, and 30 mice; s.d.). **D** Overall survival (n = 29, 12, and 33 mice). **E** *Twist1* or *Snai1 in situ* hybridization (black) with CK8 (red) immunolabeling in primary tumors (n = 3 mice for all groups) relative percentage of *Twist1*+CK8+ or *Snai1*+CK8+ double positive cells (scale, 50μm; two-tailed t-test). **F** αSMA immunolabeling in YFP lineage traced tumors (n = 3 and 3 mice; scale, 50μm; two-tailed t-test). **G** αSMA (red),

CK8 (green) and DAPI (blue); white arrows indicate double positive cells (n = 4 mice for all groups; scale, 20μm). **H** Zeb1 (n = 5, 6, and 6 mice; scale, 50 μm; inset scale, 20 μm). **I** Masson's Trichrome Stain (MTS) (n = 8, 7, and 7 mice; scale, 200 μm; s.d.). Unless otherwise indicated error bars represent s.e.m, percentages represent percent change from control and significance determined by oneway ANOVA. *P< 0.05, ** P<0.01, *** P <0.001, **** P<0.0001. *ns*, not significant.
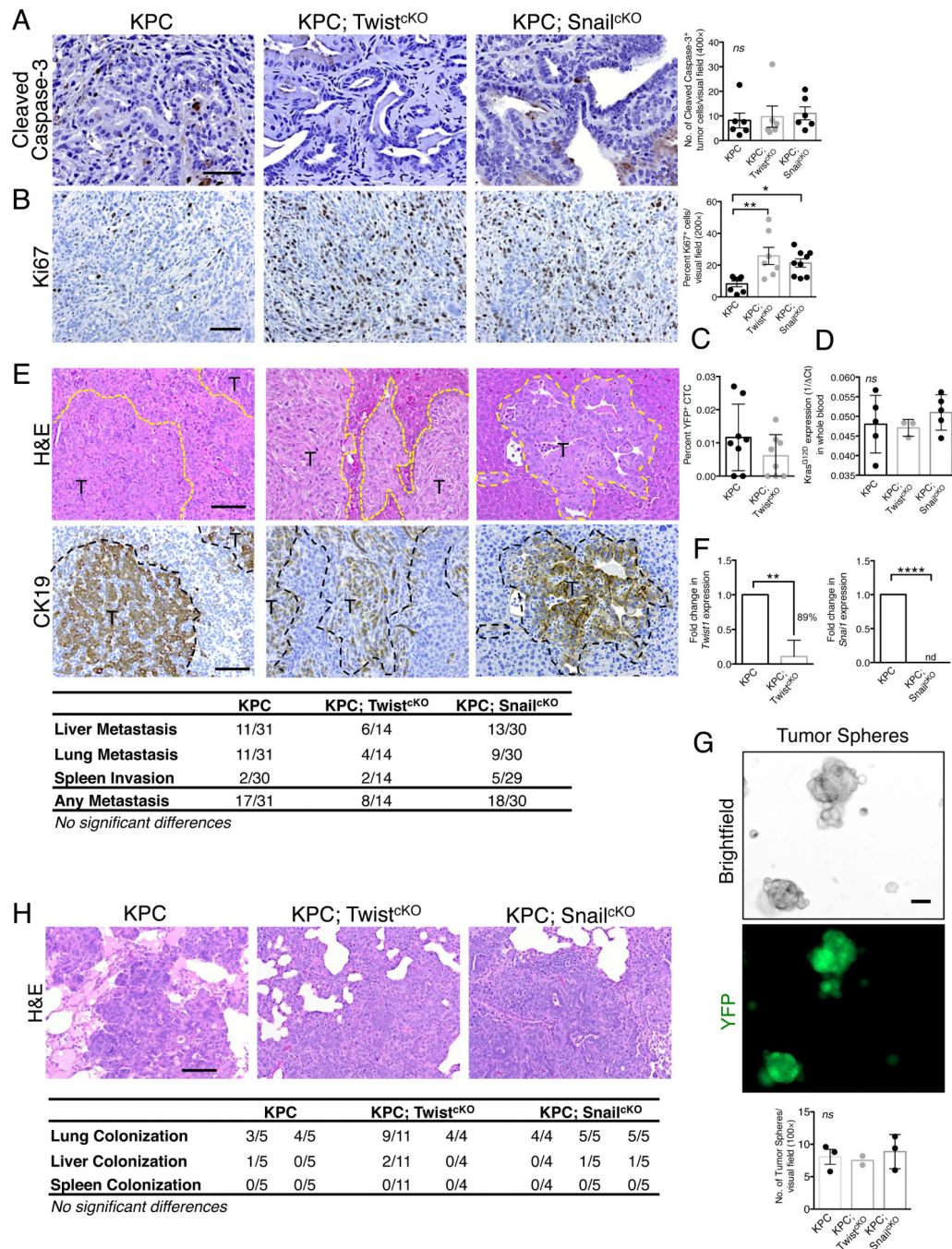
Figure 2. EMT inhibition does not alter invasion and metastasis

Primary tumor immunolabeling for (**A**) Cleaved caspase-3 (n = 6 mice for all groups; scale, 50μm) and (**B**) Ki-67 (n = 7, 7, and 9 mice; scale, 100 μm). **C** Percentage of YFP[+] circulating tumor cells (CTC) (n = 8 and 8 mice; two-tailed t-test; s.d.). **D** Kras[G12D] expression in whole blood cell pellets (n = 5, 3, and 5 mice; s.d.). **E** H&E and CK19 immunolabeling of metastatic liver nodules. Metastatic tumor (T) nodules outlined by a dotted line (scale, 100μm). Table representing the number of positive tissues out of total tissues examined (χ[2] analysis). **F** Expression analysis of *Twist1* and *Snai1* in cultured

primary tumor cell lines (n = 4 and 5 or 4 and 6 individual cell lines; one-tailed t-test of Ct; s.d.). **G** Brightfield or YFP images and quantification of sphere number in cultured tumor cell lines (n = 3, 2, and 3 individual cell lines; scale, 50μm). **H** H&E images (scale, 100μm) of colonized lungs from i.v. injected cultured primary tumor cell lines KPC (n = 5 and 5 mice for each cell line) and KPC; Twist[cKO] (n = 11 and 4 mice for each cell line) and KPC; Snail[cKO] (n = 4, 5, and 5 mice for each cell line). Table representing the number of colonized tissues out of total tissues examined (χ^2 analysis). Unless otherwise indicated error bars represent s.e.m and significance determined by one-way ANOVA. * $P < 0.05$, ** $P < 0.01$, **** $P < 0.0001$. *ns*, not significant. nd, not detected.
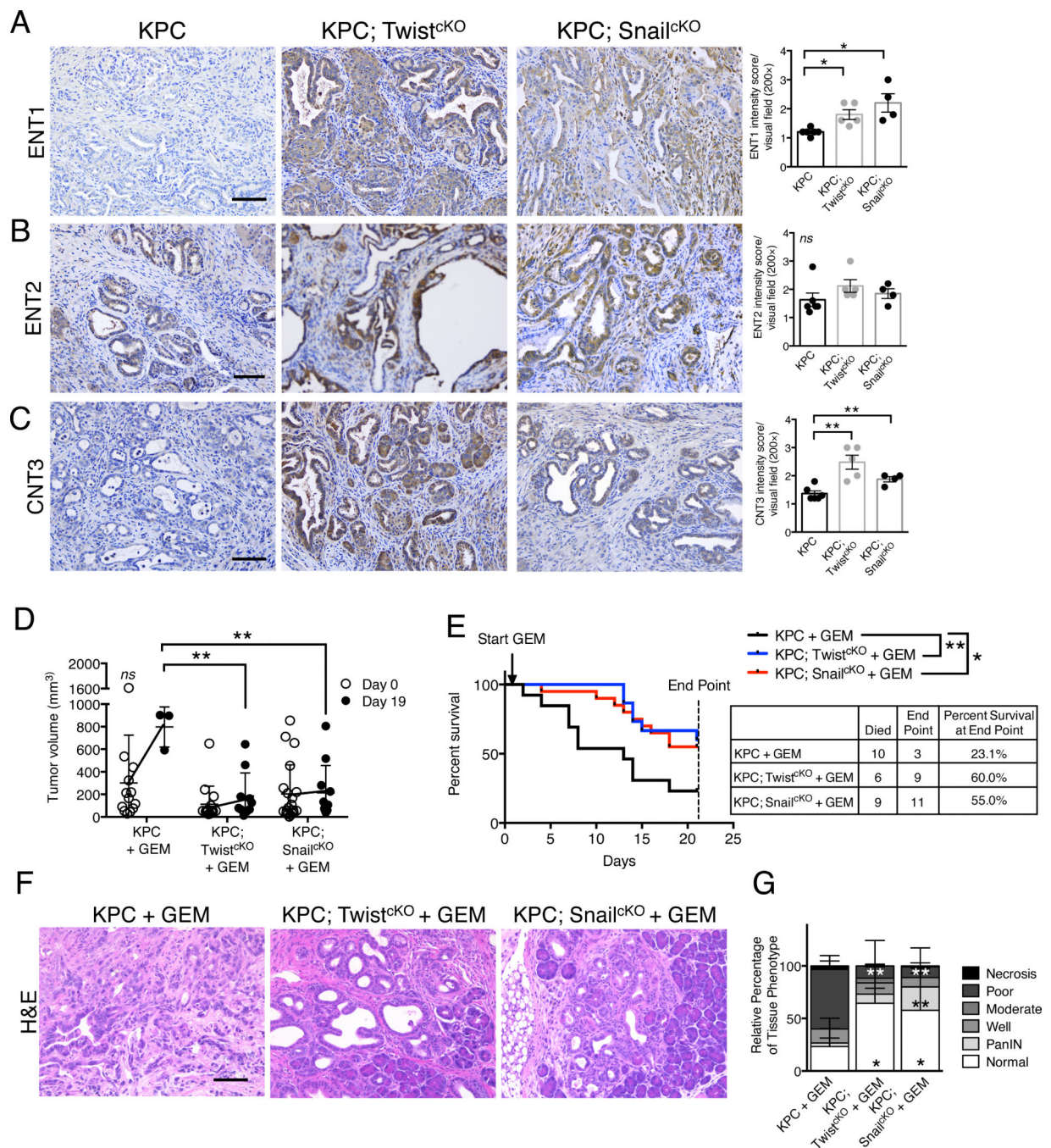
Figure 3. EMT inhibition sensitizes tumors to gemcitabine in KPC GEMM

Primary tumor immunolabeling for (**A**) ENT1, (**B**) ENT2, and (**C**) CNT3 (n = 6, 5, and 4 mice; scale, 100 μm; s.e.m., two-tailed t-test). **D** MRI tumor volumes of KPC + GEM (n = 13 mice, 10 died before Day 19), KPC; Twist^{cKO} + GEM (n = 15 mice, 6 died before Day 19) and KPC; Snail^{cKO} + GEM (n = 20 mice, 9 died before Day 19) (one-way ANOVA comparing mean tumor volumes on Day 0 and Day 19, respectively). **E** Survival on gemcitabine treatment to end point (Day 21). **F** H&E stained primary tumors (scale,
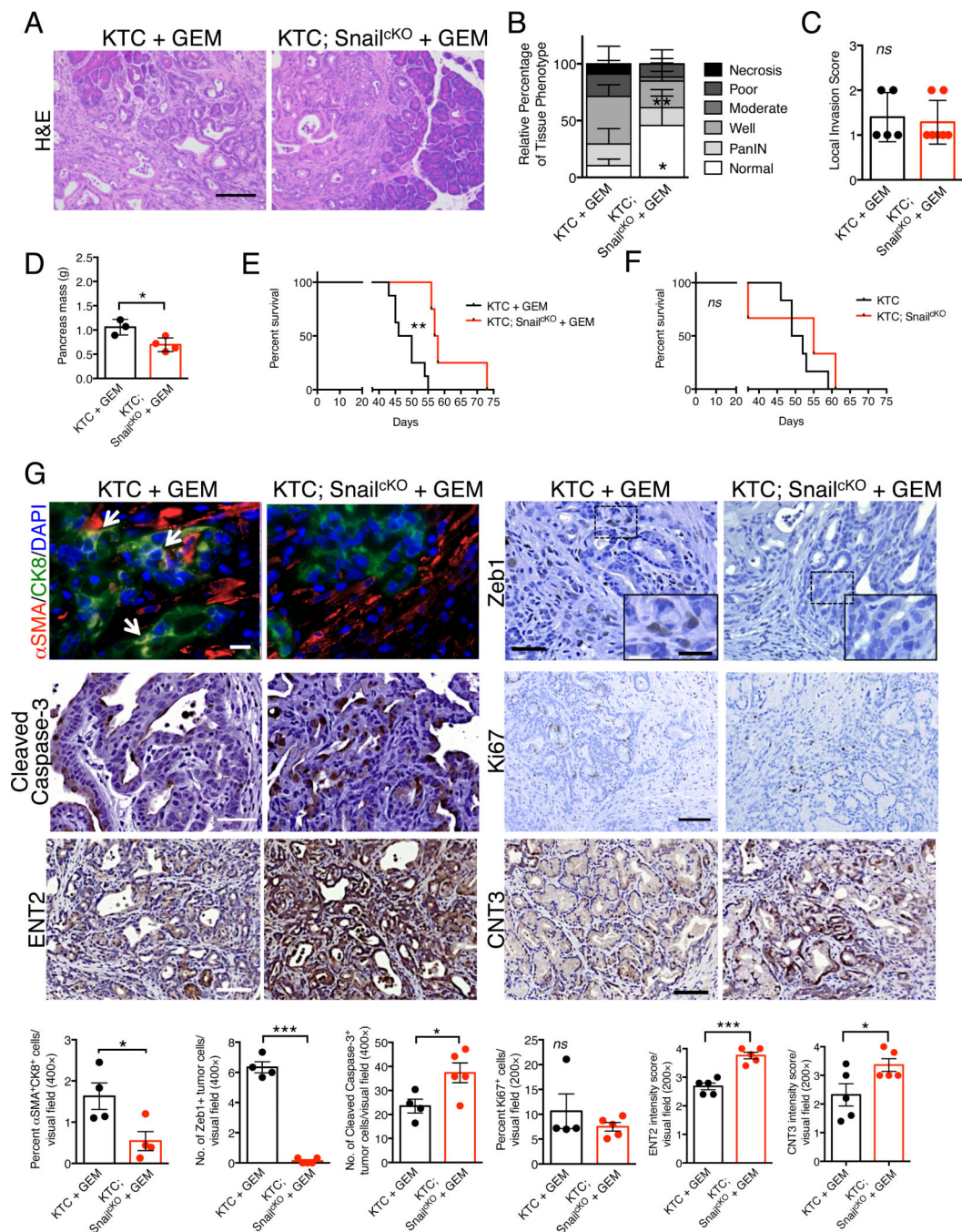
100μm). **G** Relative percentages of each histological tissue phenotype of end point mice (n = 3, 9, and 11 mice; s.d.; two-tailed t-test). * *P*<0.05, ** *P*<0.01. *ns*, not significant.

Figure 4. EMT inhibition sensitizes tumors to gemcitabine in KTC GEMM

Primary tumor (**A**) H&E (scale, 100 μm) and (**B**) relative percentage of each histological tissue phenotype (n = 5 and 7 mice; s.d.) **C** Local invasiveness (n = 5 and 7 mice; s.d.). **D** Pancreatic mass (n = 3 and 4 mice; s.d.). **E** Overall survival of KTC + GEM (n = 8 mice) and KTC; Snail^{cKO} + GEM (n = 4 mice). **F** Overall survival of KTC (n = 6 mice) and KTC; Snail^{cKO} (n = 3 mice). **G** αSMA (red), CK8 (green) and DAPI (blue); white arrows indicate double positive cells (n = 4 mice; scale, 20 μm), Zeb1 (n = 4 and 5 mice; scale, 50 μm; inset scale, 20μm), cleaved caspase-3 (n = 4 and 5 mice; scale, 50 μm), Ki-67 (n = 4 and 5 mice;

scale, 100 μm), ENT2 (n = 5 mice; scale, 100 μm), and CNT3 (n = 5 mice; scale, 100 μm). Unless otherwise indicated error bars represent s.e.m and significance determined by two-tailed t-test. * P<0.05, ** P<0.01, *** P<0.001. ns, not significant.